Intra-individual comparison of PET/CT with different body weight-adapted FDG dosage regimens

Jan H Geismar[1,2], Paul Stolzmann[1,3,4], Bert-Ram Sah[1], Irene A Burger[1,4], Burkhardt Seifert[5], Gaspar Delso[1,6], Gustav K von Schulthess[1], Patrick Veit-Haibach[1,4] and Lars Husmann[1]

Abstract

Background: 18F-2-fluoro-2-deoxy-D-glucose (FDG) positron emission tomography (PET)/ computed tomography (CT) imaging demands guidelines to safeguard sufficient image quality at low radiation exposure. Various FDG dose regimes have been investigated; however, body weight-adapted dose regimens and related image quality (IQ) have not yet been compared in the same patient.

Purpose: To investigate the relationship between FDG dosage and image quality in PET/CT in the same patient and determine prerequisites for low dosage scanning.

Material and Methods: This study included 61 patients undergoing a clinically indicated PET/CT imaging study and follow-up with a normal (NDS, 5 MBq/kg body weight [BW]) and low dosage scanning protocol (LDS, 4 MBq/kg BW), respectively, using a Discovery VCT64 scanner. Two blinded and independent readers randomly assessed IQ of PET using a 5-point Likert scale and signal-to-noise ratio (SNR) of the liver.

Results: Body mass index (BMI) was significantly lower at LDS ($P = 0.021$) and represented a significant predictor of SNR at both NDS ($P < 0.001$) and LDS ($P = 0.005$). NDS with a mean administered activity of 340 MBq resulted in significantly higher IQ ($P < 0.001$) and SNR as compared with LDS with a mean of 264 MBq (F-value $= 23.5$, $P < 0.001$, mixed model ANOVA adjusted for covariate BMI). Non-diagnostic IQ at LDS was associated with a BMI > 22 kg/m^2.

Conclusion: FDG dosage significantly predicts IQ and SNR in PET/CT imaging as demonstrated in the same patient with optimal IQ achieved at 5 MBq/kg BM. PET/CT imaging at 4 MBq/kg BW may only be recommended in patients with a BMI ≤ 22 kg/m^2 to maintain diagnostic IQ.

Introduction

The increasing use of 18F-2-fluoro-2-deoxy-D-glucose (FDG) positron emission tomography (PET)/ computed tomography (CT) imaging in cancer staging revealed a rising demand for guidelines in order to guarantee procedure safety and diagnostic quality (1). Regarding dosage regimens, different approaches exist recommending either the administration of absolute (2) or relative, i.e. body weight (BW)-adapted FDG dosages (3). The latter approach factors the need for higher

[1]Division of Nuclear Medicine, University Hospital Zurich, Zurich, Switzerland
[2]Center for Proton Therapy, Paul Scherrer Institute, Villigen, Switzerland
[3]Division of Neuroradiology, University Hospital Zurich, Zurich, Switzerland
[4]Institute of Diagnostic and Interventional Radiology, University Hospital Zurich, Zurich, Switzerland
[5]Division of Biostatistics, Institute of Social- and Preventive Medicine, University of Zurich, Switzerland
[6]GE Healthcare, Waukesha, Wisconsin, USA

Corresponding author:
Paul Stolzmann, University Hospital Zurich, Raemistrasse 100, 8091 Zurich, Switzerland.
Email: paul.stolzmann@usz.ch

administered activities in patients with an elevated body mass index (BMI) (4). Diagnostic image quality (IQ) is guaranteed and paralleled by a radiation burden which is "as low as reasonably achievable" according to the ALARA principle.

Many studies have not only explored into different acquisition parameters (5–8) but also compared the IQ of a wide range of FDG dosages (9,10). All of the aforementioned studies are, however, biased by the interindividual variability among different patient cohorts. Last but not least, there is limited agreement on the relative FDG dosage that has to be administered in BW-adapted FDG dosage regimens (3).

The aim of this study was to investigate into the relationship between FDG dosage and IQ in PET/CT in the same patient and to determine prerequisites for low dosage scanning.

Material and Methods

This single center observational cohort study was approved by the review board of our institution, and informed consent was waived due to the retrospective nature of the study.

Patients

Imaging studies obtained between November 2012 and August 2013 were reviewed to identify patients who had undergone PET/CT with normal dosage scanning (NDS), i.e. FDG-dosage of 5 MBq/kg BW ($n = 167$) and low dosage scanning (LDS), i.e. FDG-dosage of 4 MBq/kg BW ($n = 86$) during follow-up (time interval, 133 ± 63 days). Patients were included when neither electronic patient chart (i.e. abnormal laboratory findings, ultrasound, magnetic resonance imaging) nor PET/CT imaging (i.e. PET with NDS, low-dose CT for attenuation correction, and/or additional contrast-enhanced abdominal CT studies) indicated any evidence of focal or diffuse hepatic disease ($n = 73$). Patients were excluded when suffering from diabetes mellitus ($n = 11$), incidental paravenous injections ($n = 0$), or when follow-up PET/CT imaging with LDS newly demonstrated hepatic disease ($n = 1$). The final sample size consisted of 61 patients (27 women; mean age, 60 ± 14 years; age range, 25–84 years; Fig. 1). Patients suffered from head-and-neck ($n = 15$), breast ($n = 10$), lung ($n = 9$), or gastrointestinal ($n = 7$), gynecological ($n = 3$), urological cancer ($n = 1$), or melanoma ($n = 7$), lymphoma ($n = 5$), and sarcoma ($n = 4$).

PET/CT imaging

After 4 h of fasting prior to PET/CT, BW, height, and glucose levels were measured. After the intravenous injection of FDG, patients were resting for 60 min. Data were acquired on a Discovery VCT64 scanner (GE Healthcare, Milwaukee, WI, USA) employing bismuth germanate (BGO) scintillators. The patient was in supine position with arms overhead.

Low-dose CT was acquired with the following parameters: tube voltage, 140 kVp; tube current time product, 10–80 mAs/slice; pitch, 1.4; collimation, 64×0.625 mm; rotation time, 0.5 ms; and field of view (FOV), 50 cm; reconstructed slice thickness, 3.75 mm; increment, 3.0 mm. PET data were acquired using the three-dimensional (3D) mode with a fixed scan duration of 2 min per bed position. Emission data were corrected for randoms, dead time, scatter, and attenuation; reconstruction was performed using a standard iterative ordered subset expectation maximization (OSEM, 8 iterations, 16 subsets) 3D algorithm; matrix size, 256×256.

Subjective IQ

Anonymized images were evaluated by two experienced readers (with 10 and 4 years of experience). Both readers blinded to patient data (i.e. glucose levels, reason of referral, dosage regimens) independently evaluated all studies in random order on a dedicated workstation (Advantage Windows, version 4.6; GE Healthcare).

Subjective IQ of axial and coronal PET/CT was rated on maximum intensity projection (MIP) of PET. Semi-quantitative assessment was performed with a 5-point Likert scale (9): score of 5, excellent IQ without any apprehensible image noise and with completely homogenous PET signal in the liver; score of 4, good IQ but locally non-uniform PET signal; score of 3, moderate IQ with image noise leading to a globally non-uniform signal reducing the confidence in the diagnostic assessment; score of 2, poor IQ with patchy signal interspaced with reduced background activity mimicking focal hepatic disease; score of 1, deficient IQ with massive signal inhomogeneity considered inadequate for any diagnostic use. Scores of 5 and 4 were considered valid for diagnostic purposes, whereas scores of 1–3 were considered of non-diagnostic quality. Exams were not repeated due to the retrospective nature of evaluation.

Objective IQ

Objective IQ readout was performed 2 weeks after the subjective quality ratings. Both readers blinded to patient data and results of subjective IQ analyses independently assessed the objective IQ. Mean activity and corresponding standard deviation (SD) were measured using electronic calipers. Spherical shaped volumes of interest (VOI, 195 ± 74 mL; 51–470 mL) were placed within the liver. Maximum VOI volume and placement
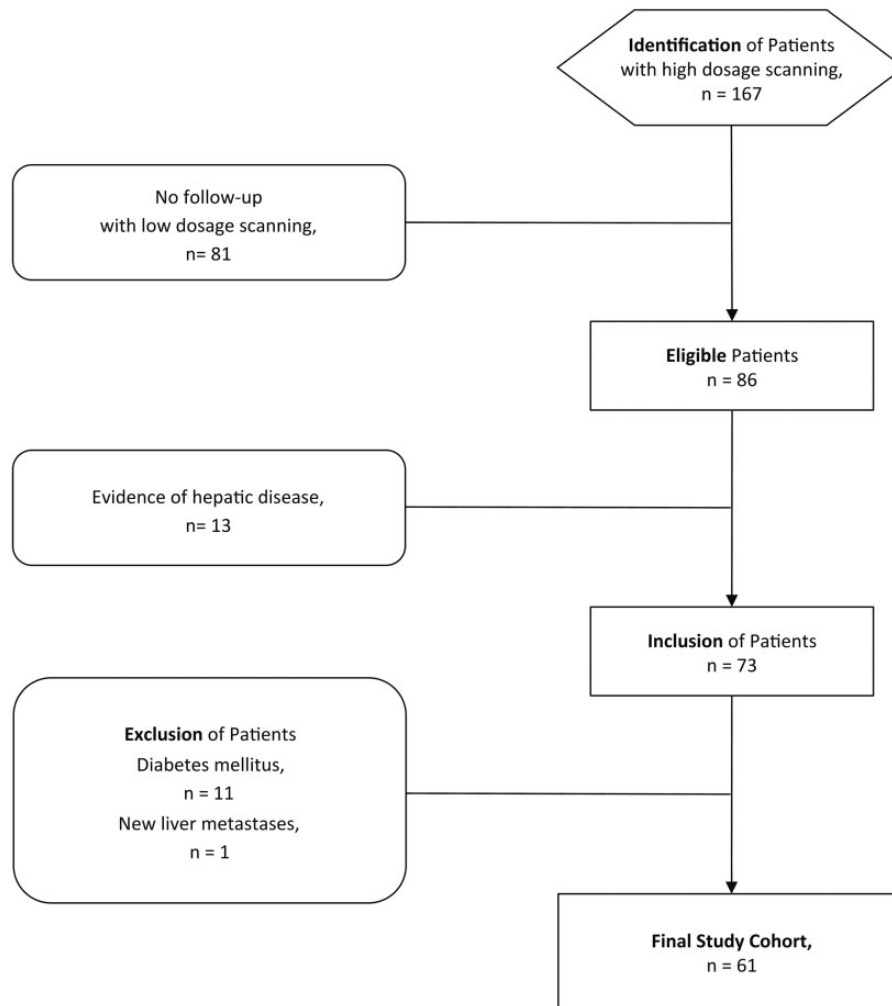
Fig. 1. Flowchart of the study design.

was confirmed on 3D reformats (11). Signal and image noise were defined as the mean activity concentration and corresponding standard deviation (SD), respectively (12). Signal-to-noise ratio (SNR) was calculated as the ratio of mean activity concentration to SD (10). SUV was not used for objective IQ measurements to avoid the effect of normalization to BW as we used a BW-adapted dose regimen.

Statistical analysis

Continuous variables were expressed as mean $\pm$ SD, categorical variables as frequencies and percentages. The Student's t-test for related samples was used to assess for any change in patient demographics.

To test for inter-reader agreement, measurements of both readers were compared. Consensus reading was appended in any case of disagreement. To test for intra-reader agreement of subjective and objective IQ-ratings, respectively, the first author re-evaluated 20

randomly selected imaging studies 6 weeks after the initial readout to avoid memory bias. Because of the excellent inter-reader agreement, mean measurements were taken for further analysis. The intra- and inter-reader agreements regarding subjective and objective IQ were analyzed by *kappa*-statistics and intra-class correlation coefficients (ICC), respectively (13).

Subjective IQ between NDS and LDS was compared with using the Wilcoxon signed rank test. Differences in objective IQ were assessed using the Student's t-test for related samples. Correlation between subjective IQ and SNR was evaluated using the Spearman's rank test.

A mixed model ANOVA was performed to assess the dependency of SNR from FDG dosage before and after adjustments for significant covariates (i.e. BMI as demonstrated during univariate testing) and the patient as a random factor.

A P value of < 0.05 was considered statistically significant. Statistical analyses were performed using commercially available software (IBM SPSS Statistics,

Version 21.0. IBM Corp., Armonk, NY, USA). Relationships of SNR and BMI at NDS and LDS were evaluated using smooth functions with automatic smoothing parameter selection using package mgcv for R (14).

Results

Patients

Mean FDG activity and blood glucose levels at LDS did not significantly (both $P > 0.05$) differ from those at NDS. The mean BMI was significantly ($P < 0.05$) lower at LDS as compared with NDS (Table 1).

Subjective IQ reading

The intra-reader agreement was high ($kappa = 0.84$, $P < 0.001$), inter-reader agreement was substantial ($kappa = 0.68$, $P = 0.002$).

NDS resulted in excellent imaging quality in 40/61 patients (66%) and good IQ in 21/61 patients (34%, Fig. 2). LDS resulted in an excellent IQ in 10/61 patients (16%), good IQ in 37/61 patients (61%), moderate IQ in 13/61 patients (21%), poor IQ in 1/61 patients (2%). IQ was significantly ($P < 0.001$) better at NDS as compared with LDS. All of the studies had diagnostic IQ at NDS, whereas a total of 14/61 studies (23%) at LDS demonstrated non-diagnostic IQ (Fig. 3) with all of the latter occurring in patients with BMI > 22 kg/m^2 ($n = 29$, 48%). In all patients with BMI < 21.8 kg/m^2, IQ was diagnostic at LDS (Fig. 4).

Objective IQ

Both intra- and inter-reader agreement was excellent regarding signal (both ICC = 0.99, $P < 0.001$) and noise measurements (ICC = 0.95 and ICC = 0.90, respectively, both $P < 0.001$).

There was a significant ($P < 0.001$) correlation between subjective IQ and SNR (rho = 0.32).

The mean signal was 7.1 ± 1.4 kBq/mL (range, 4.0–11.4 kBq/mL) at NDS and 5.7 ± 1.2 kBq/mL (range, 3.1–8.8 kBq/mL) at LDS. Mean noise was 1.0 ± 0.1 kBq/mL (range, 0.7–1.3 kBq/mL) at NDS and 0.9 ± 0.2 kBq/mL (range, 0.5–1.2 kBq/mL) at LDS. The mean SNR was 7.4 ± 1.3 (range, 4.8–10.7) at NDS and 6.8 ± 1.1 (range, 4.1–9.6) at LDS (Fig. 5). Signal and SNR were significantly (both $P < 0.001$) higher at NDS than at LDS. The correlation between SNR and BMI was significant at NDS ($P < 0.001$) and LDS ($P = 0.005$).

Multivariate analyses demonstrated FDG dosage regimens to significantly predict SNR in PET/CT imaging. The F-value for LDS vs. NDS increased after adjustments for the significant covariate of BMI was performed (Table 2). When plotting the SNR to the BMI, flattening curves were noted with minimal turning points at a BMI of 24.3 kg/m^2 and 22.1 kg/m^2 at NDS and LDS, respectively (Fig. 6a and b).

Discussion

Our results demonstrate an optimal IQ at NDS with 5 MBq/kg BW. IQ at LDS was significantly inferior but maintained in smaller patients. This is underlined by the fact that the BMI represents a significant predictor of IQ. Therefore, we suggest a cutoff level of a BMI smaller than 22 kg/m^2 to use a LDS protocol with 4 MBq/kg BW. This similarly minimizes the number of PET/CT studies with non-diagnostic IQ as well as the radiation burden due a by 20% reduced administered activity.

Although IQ has been demonstrated to behave dosage dependent (10), to the best of our knowledge, there are no studies which factored the high inter-subject variability of patients. In our study, the same patient underwent both NDS and LDS for a valid comparison of different dosage regimens.

Table 1. Patient and protocol parameters at normal (NDS) and low dosage scanning (LDS).

	NDS	LDS	P value
Mean FDG activity administered (MBq)	340 ± 24 (217–404)	264 ± 33 (215–361)	0.001
Uptake time (min)	60.3 ± 2.1 (56–69)	60.2 ± 5.1 (38–79)	0.936
Mean blood glucose levels (mmol/L)	5.6 ± 0.8 (4.2–7.7)	5.6 ± 0.8 (3.9–7.9)	0.603
Body weight (kg)	65.2 ± 9.8 (36–80)	64.2 ± 9.7 (43–81)	0.013
Body height (cm)	169 ± 8 (149–188)	169 ± 8 (149–188)	1.000
BMI (kg/m^2)	22.8 ± 3.1 (16.0–32.1)	22.4 ± 3.0 (17.4–32.5)	0.021
Time interval between scans	133 ± 63 (18–198)		n.a.

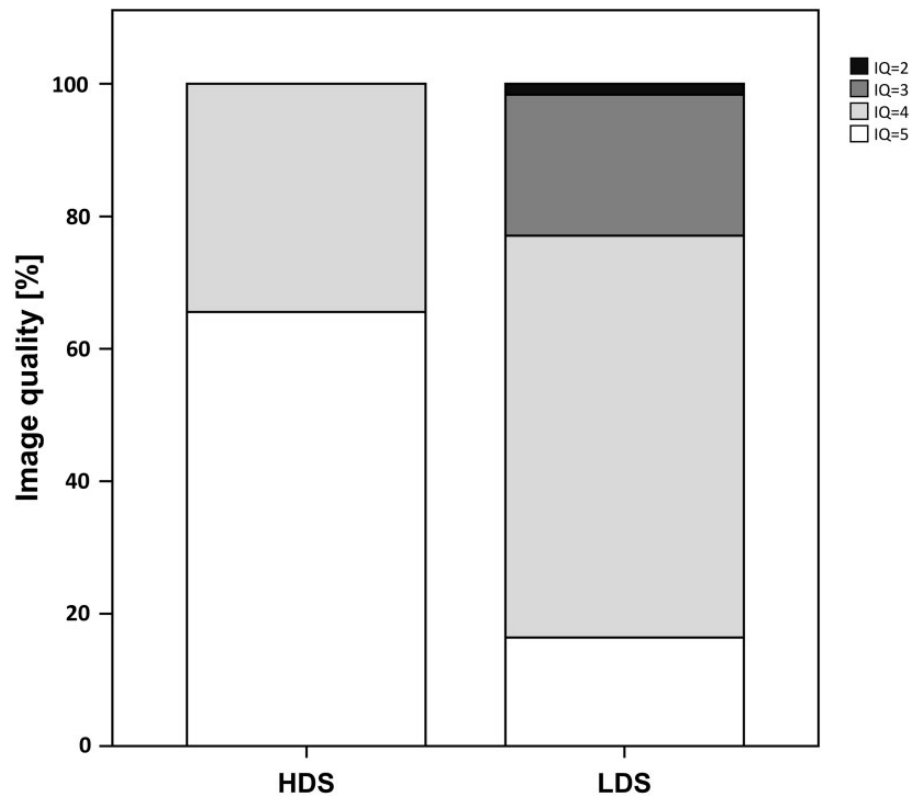BMI, body mass index; FDG, 18F-2-fluoro-2-deoxy-D-glucose; n.a., not applicable.

Fig. 2. Bar chart demonstrating percentage distribution of image quality of positron emission tomography at normal (NDS) and low dosage scanning (LDS). Note the significant ($P < 0.001$) decrease of image quality at LDS.
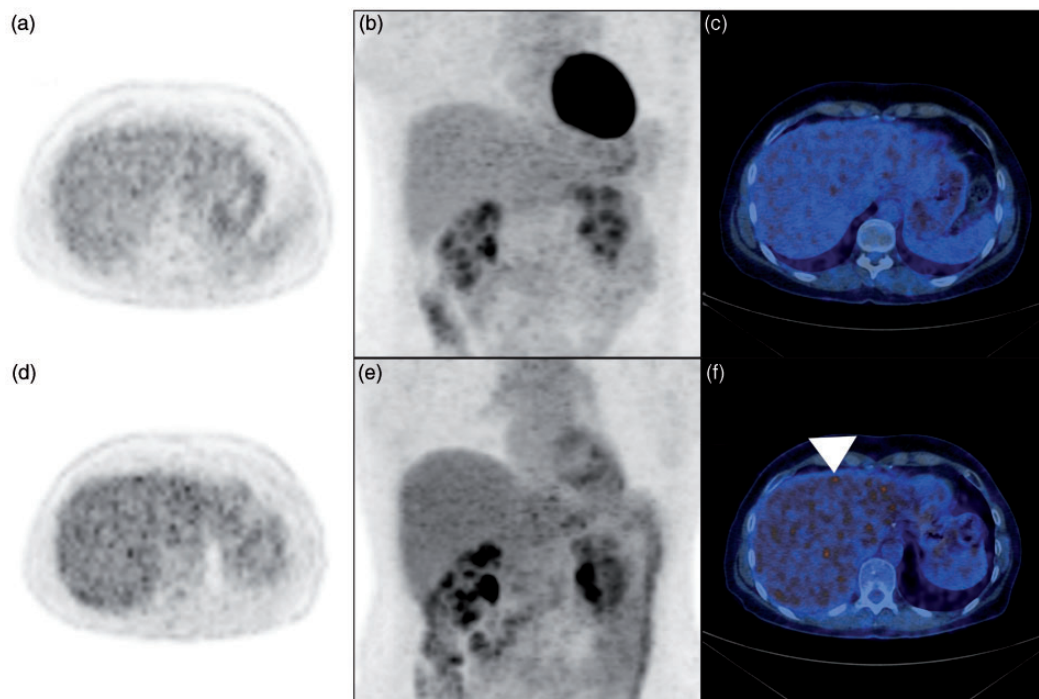

Fig. 3. A 55-year-old female patient suffering from gastric cancer having a BMI of 27 kg/m^2 at NDS and 23 kg/m^2 at LDS. (a) Axial PET image, (b) PET coronal maximum intensity projection, and (c) fused PET/ CT image acquired at 5 MBq/kg BW (i.e. NDS) similarly demonstrate diagnostic image quality. Corresponding (d) axial PET image, (e) coronal maximum intensity projection, and (f) fused PET/ CT image acquired at 4 MBq/kg BW (i.e. LDS) indicate non-uniform signal distribution that is most pronounced in the center and the left hepatic lobe. Note focal signal inhomogeneity mimicking focal uptake (f, arrowhead) that may reduce the confidence in diagnostic assessment.
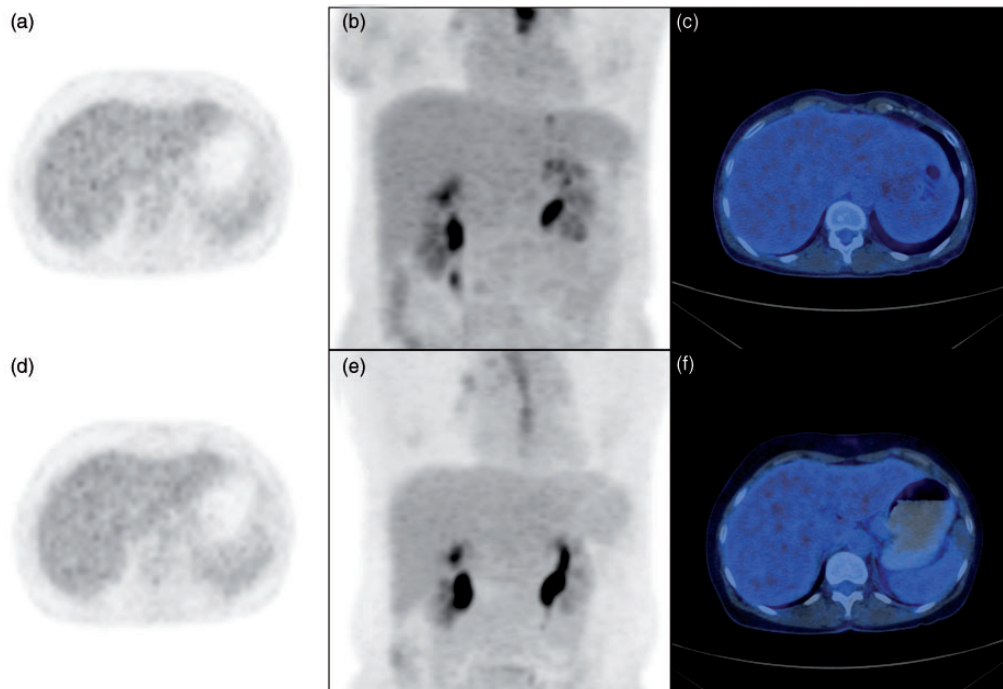
Fig. 4. A 51-year-old female patient with the history of esophageal cancer and body mass index of $16 \, kg/m^2$ at NDS and $19 \, kg/m^2$ at LDS. (a) Axial PET image, (b) coronal maximum intensity projection, and (c) fused PET/CT image acquired at 5 MBq/kg BW (i.e. NDS) demonstrate excellent image quality. Corresponding (d) axial PET image, (e) coronal maximum intensity projection, and (f) fused PET/CT image acquired at 4 MBq/kg BW (i.e. LDS) similarly demonstrate excellent image quality with completely homogenous PET signal in the liver. Note that the diagnostic image quality is maintained with a BMI $< 22 \, kg/m^2$.
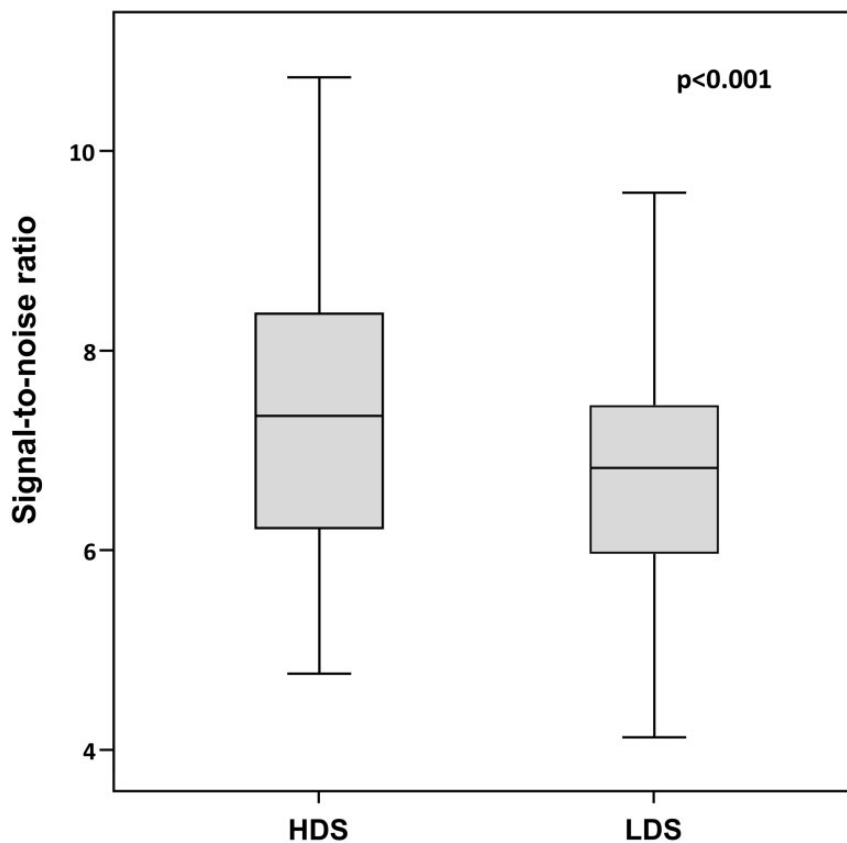

Fig. 5. Box plots demonstrating the signal-to-noise ratio at NDS and LDS. Note the significant ($P < 0.001$) higher SNR with NDS as compared with LDS.

Table 2. Multivariate models for the prediction of objective image quality in PET.

	F-value	P value
(a) Model for signal-to-noise ratio		
Normal vs. low dosage scanning	20.3	<0.001
(b) Model for signal-to-noise adjusted for BMI		
Normal vs. low dosage scanning	23.5	<0.001
Body mass index (kg/m^2)	2.72	0.104

Higher F-value after adjustment for the covariate body mass index that decreased significantly after high and prior to low dosage scanning.

Subjective IQ was significantly improved with NDS as compared with LDS. This subjective IQ was significantly correlated with the objective IQ measurements. This, however, may only hold true within certain ranges since the human eye fails to appreciate reduced noise levels beyond certain thresholds. Therefore, images were evaluated by means of both objective and subjective parameters.

A significant decrease in BMI was noted between NDS and LDS. Thus, statistical testing was corrected for BMI. When plotting the SNR to BMI, flattening of curves were found at both NDS and LDS with minimal
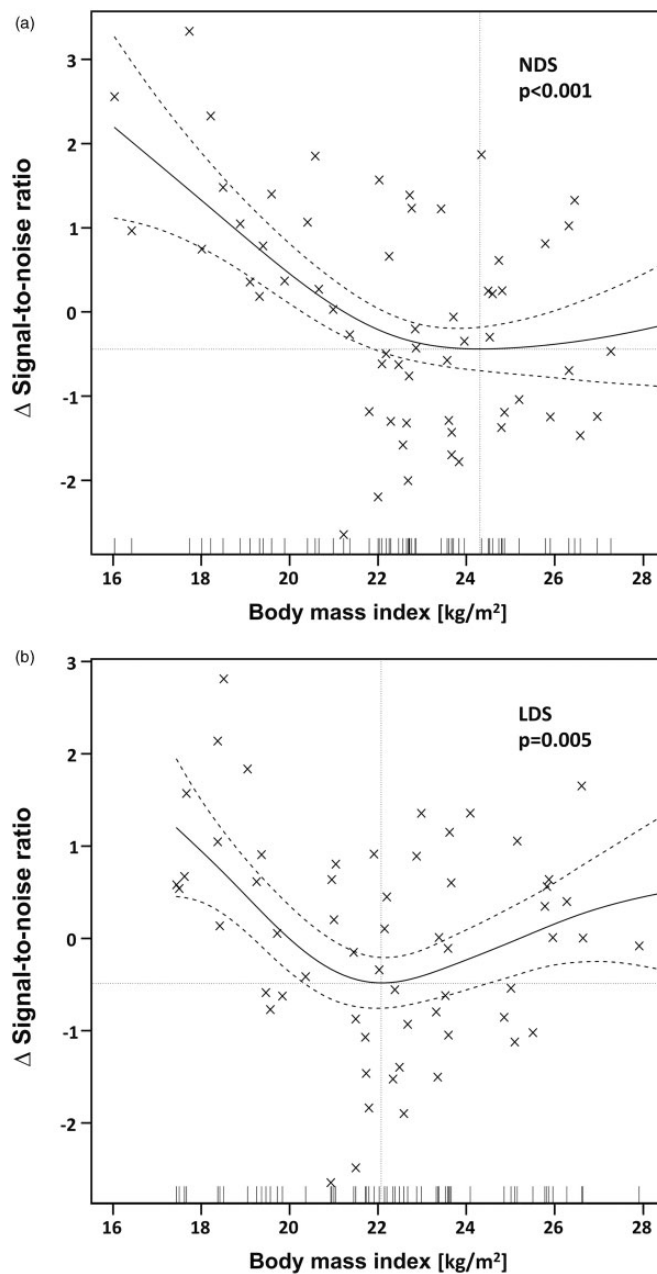

Fig. 6. Scatter plots with smoothed functions (solid curves) and 95% confidence intervals (dashed curves) demonstrating the relationship between SNR and BMI at (a) NDS and (b) LDS. Δsignal-to-noise ratio represents the difference from the mean signal to noise and allows for a valid comparison of dependencies of SNR on BMI and thus optimal comparison among groups. Note the flattening curves with increasing body mass indices and minimal turning points (dotted lines) at 24.3 kg/m^2 at NDS and 22.1 kg/m^2 at LDS.

turning at $24 \, \text{kg/m}^2$ and $22 \, \text{kg/m}^2$, respectively. These turning points represent the more than linear increased attenuation of photon transmission in larger patients (10). As a cutoff, we suggest a BMI value of $22 \, \text{kg/m}^2$ to change from LDS to NDS on the bases of subjective and objectives IQ.

The suggested cutoff value represents a valid suggestion for daily practice; however, several factors impacting on PET IQ have to be considered (1,9,15,16). Scanner performance may for instances be enhanced by improved system geometry and novel non-photo-multiplier based detectors (17) and time-of-flight imaging (7,18). Different reconstruction parameters exist and IQ may further be improved by applying modifications to raw data or changing properties in the image domain (19).

Finally, the noise equivalent count rate (NECR) represents a machine dependent quality measure of PET raw data (20) that is strongly related to image noise and SNR in the reconstructed image (21,22). This allows for a comparison of IQ among PET machines, which is facilitated when the NECR is plotted to activity concentrations (23). In detail, a distinct NECR is found at different activity concentrations when various machines are used. If equal reconstruction parameters are selected, the recommended activity cutoff values for the Discovery VCT machine may be corrected for other target scanners accordingly (23).

We acknowledge the following limitations. We did not adjust for potential longitudinal scanner variability but routinely performed quality assurance and control procedures (24). We did not consider increasing acquisition times per bed position as a parameter for noise reduction as examination times are valuable and cannot be overly extended (25). Respiratory gating is known to attenuate PET/CT imaging artifacts (26), improves IQ which may translates into improved detection of lung and liver lesions (27), but is not routinely performed. Lesion detection or conspicuity was not assessed as patients with liver lesions were excluded from our study to overcome bias from confounding factors, e.g. tumor progression and/or treatment. Therefore, the risk of missing lesions at LDS could not be assessed and has to be put in relation to benefits of a reduced risk for secondary cancer from radiation dose exposure. No *in-vivo* dosimetry was performed to quantify the patient's radiation exposure at LDS and NDS. Last but not least, our results are derived from a certain scanner type only but we provide a theoretical method for transferability by means of NECR to other machine types.

In conclusion, administered FDG activity significantly predicts subjective IQ and SNR in PET/CT as demonstrated in the same patient. Our data derived from both subjective and objective measurements both suggest BMI-based cutoff values for choosing FDG dosages to maintain diagnostic IQ. Given the used imaging setting, an optimal IQ was achieved at 5 MBq/kg BW, whereas PET/CT imaging at 4 MBq/kg BW can only be recommended in patients with a BMI smaller than $22 \, \text{kg/m}^2$.

Conflict of interest

References

1. Boellaard R. Standards for PET image acquisition and quantitative data analysis. J Nucl Med 2009;50(Suppl. 1): 11S–20S.
2. American College of Radiology. ACR-SPR practice parameter for performing FDG-PET/CT in oncology. Reston, VA: American College of Radiology; 2014. Available at: http://www.acr.org/~/media/ACR/Documents/PGTS/guidelines/FDG_PET_CT.pdf.
3. Boellaard R, O'Doherty MJ, Weber WA, et al. FDG PET and PET/CT: EANM procedure guidelines for tumour PET imaging: version 1.0. Eur J Nucl Med Mol Imaging 2010;37:181–200.
4. Tatsumi M, Clark PA, Nakamoto Y, et al. Impact of body habitus on quantitative and qualitative image quality in whole-body FDG-PET. Eur J Nucl Med Mol Imaging 2003;30:40–45.
5. Akamatsu G, Ishikawa K, Mitsumoto K, et al. Improvement in PET/CT image quality with a combination of point-spread function and time-of-flight in relation to reconstruction parameters. J Nucl Med 2012;53: 1716–1722.
6. Halpern BS, Dahlbom M, Quon A, et al. Impact of patient weight and emission scan duration on PET/CT image quality and lesion detectability. J Nucl Med 2004;45:797–801.
7. Akamatsu G, Mitsumoto K, Ishikawa K, et al. Benefits of point-spread function and time of flight for PET/CT image quality in relation to the body mass index and injected dose. Clin Nucl Med 2013;38:407–412.
8. Cheng G, Alavi A, Werner TJ, et al. Serial changes of FDG uptake and diagnosis of suspected lung malignancy: a lesion-based analysis. Clin Nucl Med 2014;39:147–155.
9. Everaert H, Vanhove C, Lahoutte T, et al. Optimal dose of 18F-FDG required for whole-body PET using an LSO PET camera. Eur J Nucl Med Mol Imaging 2003;30: 1615–1619.
10. de Groot EH, Post N, Boellaard R, et al. Optimized dose regimen for whole-body FDG-PET imaging. EJNMMI Res 2013;3:63.
11. Soret M, Bacharach SL, Buvat I. Partial-volume effect in PET tumor imaging. J Nucl Med 2007;48:932–945.

12. Lodge MA, Rahmim A, Wahl RL. Simultaneous measurement of noise and spatial resolution in PET phantom images. Phys Med Biol 2010;55:1069–1081.
13. Landis JR, Koch GG. The measurement of observer agreement for categorical data. Biometrics 1977;33:159–174.
14. R Development Core Team. R: A language and environment for statistical computing. Vienna: R Foundation for Statistical Computing; 2011. Available at: http://www.R-project.org.
15. Boellaard R, Krak NC, Hoekstra OS, et al. Effects of noise, image resolution, and ROI definition on the accuracy of standard uptake values: a simulation study. J Nucl Med 2004;45:1519–1527.
16. Kinahan PE, Fletcher JW. Positron emission tomography-computed tomography standardized uptake values in clinical practice and assessing response to therapy. Semin Ultrasound CT MR 2010;31:496–505.
17. Peng BH, Levin CS. Recent development in PET instrumentation. Curr Pharm Biotechnol 2010;11:555–571.
18. Hausmann D, Bittencourt LK, Attenberger UI, et al. Diagnostic accuracy of 18F choline PET/CT using time-of-flight reconstruction algorithm in prostate cancer patients with biochemical recurrence. Clin Nucl Med 2014;39:e197–201.
19. Lee K, Miyaoka RS, Lewellen TK, et al. Impact on image noise of incorporating detector blurring into image reconstruction for a small animal PET scanner. IEEE Trans Nucl Sci 2009;56:2769–2776.
20. McDermott GM, Chowdhury FU, Scarsbrook AF. Evaluation of noise equivalent count parameters as indicators of adult whole-body FDG-PET image quality. Ann Nucl Med 2013;27:855–861.
21. Chang T, Chang G, Kohlmyer S, et al. Effects of injected dose, BMI and scanner type on NECR and image noise in PET imaging. Phys Med Biol 2011;56:5275–5285.
22. Matsumoto K, Shimizu K, Kitamura K, et al. Comparison of noise equivalent count rate and image quality for two-dimensional and three-dimensional PET scans. Nihon Hoshasen Gijutsu Gakkai Zasshi 2006;62:1111–1118.
23. Teras M, Tolvanen T, Johansson JJ, et al. Performance of the new generation of whole-body PET/CT scanners: Discovery STE and Discovery VCT. Eur J Nucl Med Mol Imaging 2007;34:1683–1692.
24. Lockhart CM, MacDonald LR, Alessio AM, et al. Quantifying and reducing the effect of calibration error on variability of PET/CT standardized uptake value measurements. J Nucl Med 2011;52:218–224.
25. Masuda Y, Kondo C, Matsuo Y, et al. Comparison of imaging protocols for 18F-FDG PET/CT in overweight patients: optimizing scan duration versus administered dose. J Nucl Med 2009;50:844–848.
26. Sureshbabu W, Mawlawi O. PET/CT imaging artifacts. J Nucl Med Technol 2005;33:156–161. (quiz 163–154).
27. Revheim ME, Haugvik SP, Johnsrud K, et al. Respiratory gated and prolonged acquisition 18F-FDG PET improve preoperative assessment of colorectal liver metastases. Acta Radiol2014;DOI: 10.1177/0284185114529563).